CRYSTAL GROWTH & DESIGN

ARTICLE

pubs.acs.org/crystal

Crystallization, Polymorphism, and Binary Phase Behavior of Model Enantiopure and Racemic Triacylglycerols

R. John Craven and Robert W. Lencki*

Department of Food Science, University of Guelph, Guelph, Ontario, Canada

ABSTRACT: Triacylglycerols (TAG) are the main component in fats and oils and a major component in many food and consumer products. These compounds are always asymmetric (about the *sn*-2 position), while many diacid and all triacid TAG are chiral. To understand what effect this has on their crystallization behavior, model enantiopure (1,2-bisdecanoyl-3-palmitoyl-*sn*-glycerol) and racemic (bisdecanoyl-1(3)-palmitoyl-*rac*-glycerol) TAG were prepared and characterized. In addition, a binary phase diagram was prepared to investigate their phase behavior and the racemate's crystalline tendency. For the subject compounds, infrared spectroscopy and X-ray powder diffraction data indicate the enantiopure TAG is β'-stable, whereas the racemic mixture is β-stable. In addition, based on the phase diagram, the high-melting form of the racemic mixture is a racemic compound (with a unit cell containing equal quantities of both enantiomers). Racemic (and near-racemic) mixtures also crystallize in a lower-melting metastable conglomerate β' form. Thus, there are critical differences between the crystallization behavior of enantiopure and racemic TAG, and future investigations of these compounds should reflect these findings.

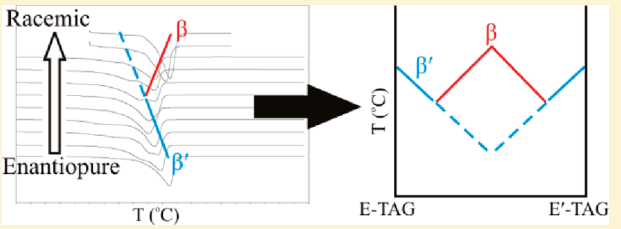

INTRODUCTION

Triacylglycerols (TAG) are the main components in fats and oils, and their crystallization behavior is of both commercial and academic interest. TAG incorporated in food and consumer products is typically from natural sources and is often chiral due to the positional specificity of biosynthetic pathways. Milk fat, with less than a handful of achiral TAG among the >300 species identified so far, is the most dramatic example of this.[1] Likewise, 15 of the 25 main TAG in palm oil are also chiral.[2] Despite remarkable differences in crystalline tendency between pure enantiomers and enantiomeric mixtures in other systems, the possibility of a similar tendency for TAG has not been explored.[3]

In the solid phase, racemic mixtures form either racemic compounds, where the unit cell contains both enantiomers; conglomerates, which are mechanical mixtures of enantiopure crystals (i.e., heterogeneous mixtures that are, in principle, separable by mechanical means); or pseudoracemates, which are solid solutions with no regular pattern.[3] Each of these crystal tendencies has their own distinct phase diagram (typically constructed using binary mixtures of enantiopure compound and racemic mixture) (Figure 1). Crystalline tendency also provides information on the stereochemistry of the unit cell configuration (i.e., equal number of opposing enantiomers for a racemic compound, single or multiple enantiopure molecules for a conglomerate, and undefined for a pseudoracemate). In combination with single-crystal X-ray data, this information can be used to determine the absolute configuration of the unit cell.

Typically, pure TAG crystallize in one of three monotropic polymorphs that are designated α, β', and β in order of increasing thermodynamic stability.[4] Polymorphism is attributed to differences in subcell structure reflected in the distance between methylene units of adjacent acyl chains as measured by X-ray diffraction (4.15 Å for α; 4.2 and 3.8 Å for β'; and 4.6, 3.9, and 3.8 or 3.7 Å for β).[5−8] In addition, solid TAG adopt one of several possible chain length (double or triple chain length aka 2L or 3L) and glycerol conformation (chair or tuning fork) structures. These structures are determined to a large part by the TAG's substituent fatty acids and their relative affinity for each other, with acyl chains congregating due to similarities in length and degree of saturation.[4] Consequently, a difference in chain length of more than 4 carbons in any one fatty acid leads to a 3L structure.[9] As a result, TAG polymorphism can be quite complex. For example, dilauroyl-1(3)-stearoyl-*rac*-glycerol crystallizes in α, β'_2, β'_3, and β_3 forms with melting points of 21.0, 31.0, 38.0, and 44.6 °C, respectively (subscripts refer to 2L and 3L structures).[9]

Historically, positional isomers of TAG have been defined as symmetric or asymmetric (e.g., 1,3-dipalmitoyl-2-oleoyl-glycerol versus 1,2-dipalmitoyl-3-oleoyl-*sn*-glycerol). Differences in the speed of polymorphic transitions and size of crystallization enthalpies between symmetric and asymmetric TAG were reported as early as 1954.[10] Similarly, differences in polymorphism between symmetric and asymmetric TAG have been remarked upon recently.[5] In reality, there are no symmetric TAG since all TAG are asymmetric about the *sn*-2 position of glycerol. Moreover, TAG previously described as asymmetric are in fact chiral and, depending on the source or means of preparation, range in composition from enantiopure to a racemic

Received: December 13, 2010
Revised: March 10, 2011
Published: March 23, 2011

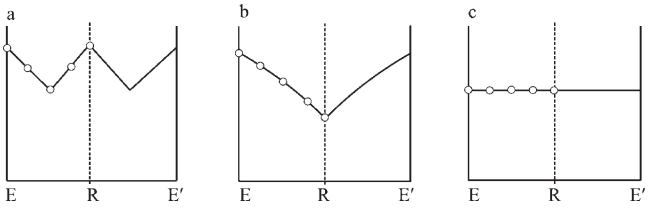

Figure 1. Characteristic liquidus lines for phase diagrams of (a) racemic compounds, (b) conglomerates, and (c) pseudoracemates (ideal behavior). Binary mixtures of an enantiopure compound (E) and racemic mixture (R) are used to prepare half of the curve. Data can be extrapolated to include the opposite enantiomer (E′) if desired.

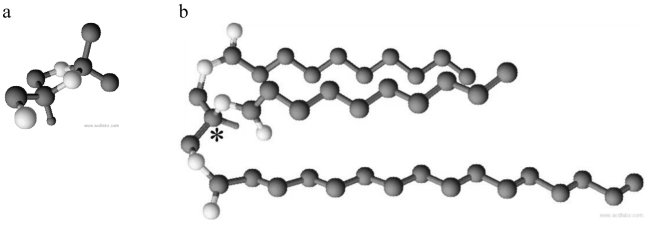

Figure 2. Stereochemistry of (a) (*S*)-1,2-isopropylidene glycerol and (b) (*R*)-1,2-bisdecanoyl-3-palmitoyl-*sn*-glycerol. Chiral carbon at the *sn*-2 position of glycerol is marked with an asterisk. Hydrogen atom displays stereochemistry at the *sn*-2 position.

mixture. The crystallization and polymorphism of enantiopure TAG and their binary mixtures has not previously been published.

The main purpose of this work is to compare the physical chemistry of an enantiopure TAG with its racemic counterpart. This will improve understanding of the role stereochemistry plays in crystallization and perhaps lend some insight into the polymorphism of TAG. 1,2-Bisdecanoyl-3-palmitoyl-*sn*-glycerol and bisdecanoyl-1(3)-palmitoyl-*rac*-glycerol were chosen as models for study because the difference in chain length was regarded as sufficient for the potential effects of chirality to be detectable.

MATERIALS AND METHODS

Unless noted otherwise, reagents, chemicals, and enzyme were purchased from Sigma-Aldrich (Mississauga, ON) and were of the highest practical grade; solvents were purchased from Fisher Scientific (Ottawa ON) and were HPLC grade. Decanoyl chloride (10:0), palmitoyl chloride, and isopropylideneglycerol all had a declared purity ≥98%. Enantiopure 1,2-isopropylideneglycerol was 99.96% pure (by GC) and had an optical purity of 99.8% according to the certificate of analysis (available from Sigma Aldrich; product number 237744; lot number 1328499). The vinyl ester of palmitic acid donated by Japan VAM & POVAL (Osaka, JP) was ≥96% purity. Prior to analysis, pure TAG were crystallized and tempered by holding isothermally at 25 °C for more than 28 days to ensure formation of the highest-melting form. These tempered samples were used for gas chromatographic analysis, infrared and X-ray spectroscopy, and differential scanning calorimetry experiments. Binary mixtures of TAG were stored at 22 °C for 3 days prior to analysis.

Synthesis. *Enantiopure 3-Palmitoyl-sn-glycerol.* Palmitoyl chloride (12.5 g) was dissolved in 30 mL of methylene chloride and then added dropwise to a solution of 1,2-isopropylidineglycerol (5.0 g) (Figure 2), triethylamine (7.66 g), and *N*,*N*-dimethylaminopyridine (0.46 g) in 70 mL of methylene chloride stirred in an ice bath. After addition, the solution was stirred at room temperature (~22 °C) for an additional 3 h. The solution was then washed with brine, dried over sodium sulfate, and filtered, and the solvent was evaporated.[11,12] Free 3-palmitoyl-*sn*-glycerol was produced by gently refluxing in 100 mL of 95% ethanol with Amberlyst 15 (wet) resin.[13] The resulting MAG was purified by recrystallization first from acetone and subsequently from hexane/ethyl ether (4:1, v/v). This yielded 7.56 g of 93% 3-palmitoyl-*sn*-glycerol containing 7% 2-palmitoyl-glycerol (by GC).

Enantiopure 1,2-Bisdecanoyl-3-palmitoyl-sn-glycerol. Decanoyl chloride (3.27 g) was dissolved in 30 mL of methylene chloride and then added dropwise to a solution of 3-palmitoyl-*sn*-glycerol (2.56 g), triethylamine (2.90 g), and *N*,*N*-dimethylaminopyridine (0.18 g) in 70 mL of methylene chloride stirred in an ice bath. After addition, the solution was stirred at room temperature (~22 °C) for 24 h. Solvent was removed under vacuum, and the residue was taken back up in hexane and filtered. A total of 3.7 g of pure product (>99% by GC) was obtained by flash chromatography with hexane/ethyl acetate (10:1, v/v).

Racemic 1(3)- Palmitoyl-rac-glycerol. The vinyl ester of palmitic acid (13.4 g) and racemic isopropylideneglycerol (5.0 g) were stirred in 100 mL of chloroform containing Lipozyme immobilized lipase from *Rhizomucor miehei* (1.0 g) at room temperature (~22 °C) under nitrogen for 3 days.[14] The immobilized enzyme was then removed by filtration, and free 1(3)-palmitoyl-*rac*-glycerol was produced as for the enantiopure 3-palmitoyl-*sn*-glycerol. This yielded 7.56 g of very pure (by TLC) 1(3)-palmitoyl-*rac*-glycerol.

Racemic Bisdecanoyl-1(3)-palmitoyl-rac-glycerol. Same method as with the enantiopure 1,2-bisdecanoyl-3-palmitoyl-*sn*-glycerol but using racemic 1(3)-palmitoyl-*rac*-glycerol as a starting material. Crystallized from hexane (−20 °C) followed by flash chromatography with hexane/ethyl acetate (10:1, v/v) to yield 2.45 g of pure product (>99% by GC).

Gas Chromatography. Prepared compounds were dissolved in iso-octane and analyzed by GC/FID to determine their purity. These were eluted on a 25 m × 0.25 mm polarizable capillary column (Quadrex, Woodbridge CT).[12] The column was housed in a Hewlett-Packard 5890 (Agilent, Palo Alto CA) GC equipped with FID and on-column inlet. The inlet pressure for the carrier gas (hydrogen) was set to 15 psi, cool on-column injection was employed, and the detector was held at 370 °C. After sample injection, the oven was held at 60 °C for 2 min, then the temperature was increased to 250 at 35 °C/min, and finally the temperature was increased to 350 at 4 °C/min.

Nuclear Magnetic Resonance. Approximately 15 mg of sample for ^{1}H NMR and 100 mg for ^{13}C NMR dissolved in 750 μL of deuterated chloroform (containing 0.5% tetramethylsilane (TMS) as internal standard) was placed in a suitable NMR tube (Wilmad, Buena, NJ). NMR spectra were obtained using an Avance III 400 MHz instrument (Bruker, Billerica, MA) (^{1}H 4 scans; ^{13}C 256 scans). Chemical shifts were measured relative to TMS internal standard. NMR spectra were integrated, analyzed using 1D NMR Processor, Academic Version (ACD, Toronto), and interpreted using relevant literature.[12,15]

Infrared Spectroscopy. Data were collected using a Shimadzu IRPrestige-12 FTIR (Kyoto) equipped with a Pike MIRacle ATR sample stage (Madison, WI). Data were analyzed using the Shimadzu IR Solution 1.30 software package.

X-ray Powder Diffraction. Solid samples were ground into fine powders and applied to sample slides with a 0.2 mm deep depression (Rigaku, Tokyo, JP). An aftermarket temperature controller utilizing Peltier cooling (Electron Dynamics, Southampton UK) maintained the sample stage at 20 °C. Powder diffraction data was recorded using a Rigaku Multiflex Powder X-ray Diffractometer with a Cu Kα radiation (λ = 1.5406 Å)[16] source and a scintillation detector. Samples were scanned from 2° to 30° at 2°/min. Results were analyzed and major peaks were identified using Jade software (Materials Data, Livermore CA).

Small Angle X-ray Scattering. Samples were ground into a fine powder and sealed between sheets of Kapton. Samples were held at 20 °C in a temperature-controlled stage while data was measured from 0.7° to 4.3° for 1 h using a Nanostar SAXS (Bruker AXS, Madison WI) with Cu Kα radiation and a High Star wire-type detector.[16] Results were analyzed using Bruker AXS software version 4.1.26.

Differential Scanning Calorimetry. Crystallization and melting curves were determined using a Q1000 DSC (TA Instruments, New Castle, DE) that was calibrated following the manufacturer's recommendations with a pure indium standard and a matched pair of sapphires. The sample cell was purged with dry nitrogen flowing at 25 mL/min. Hermetically sealed alodined aluminum DSC pans containing 4−8 mg of sample were processed, and heatflow was measured relative to an empty sealed DSC pan. Results were analyzed using Universal Analysis software (TA Instruments).

DSC samples were prepared by transferring tempered solid TAG to the sample pan without melting; the initial melt of these samples was measured (at 5 °C/min). This provided the melting data (T_e, T_p, and ΔH_f) for the high-melting form of each compound. Afterward, samples were analyzed by DSC at three different cooling/heating rates (2, 5, and 10 °C/min) because DSC scans collected at several rates are useful for detecting polymorphism.[17] Universal Analysis software was used to determine the extrapolated onset of melting (T_e), peak maximum (T_p), and enthalpy (ΔH_f) of both melting and crystallization. Measurements obtained from melting curves are considered more reliable than those arising from crystallization because the latter requires undercooling and is delayed by the need for nucleation.[18] The preferred measurement of melting temperature (T_m) is the extrapolated onset of melting temperature (T_e) because it has been shown to vary the least with heating rate. T_e is the temperature at which a tangent through the linear portion of the leading edge of the peak intersects with the baseline.[17] In the event that T_e was not available, as is the case with peaks that are merged due to polymorphism, T_p is an acceptable approximation.[18,19]

Phase Diagrams. Phase diagram samples were prepared from solutions of pure compounds dissolved in chloroform/ethyl acetate (1:1). Samples with proportions 1:9 (i.e., 100 μL + 900 μL), 2:8 (i.e., 200 μL + 800 μL), 3:7, 4:6, ..., 9:1 were prepared. Solvent was evaporated under a stream of nitrogen with mild heating (∼40 °C) to compensate for enthalpy of vaporization. Once solvent had completely evaporated, melted samples were weighed into DSC pans and sealed. Samples of enantiopure and racemic TAG and a tridecanoin standard (NuChek-Prep, MN) were prepared and tested in the same manner to verify the method. DSC melting data was collected from samples with a heating rate of 2 °C/min in the manner described above. Afterward, samples were crystallized and melted at 2, 5, and 10 °C/min in a similar manner. A phase diagram was prepared by plotting the appropriate melting data as a function of composition.

Calculations. The theoretical melting point depression was calculated using a form of the Hildebrand equation:

$$\Delta T \approx \left(\frac{RT_E^2}{\Delta H_f}\right) \ln \gamma x \qquad (1)$$

where ΔT is the melting point depression, T_E (in Kelvin) is assumed to approximately equal to T_R, and γ is assumed to be one.[20] The molar enthalpy of formation for the racemic compound from pure crystalline enantiomers was calculated using

$$-\Delta H_f^{\phi} = \Delta H_E - \Delta H_R + (C_l - C_S^R)(T_R - T_E) \qquad (2)$$

where all enthalpy and temperature values are for fusion, C is the molar heat capacity at constant pressure, and temperature is in Kelvin.[3] The molar entropy of formation for the racemic compound from pure crystalline enantiomers was calculated using

$$\Delta S_f^{\phi} = \Delta S_E - \Delta S_R + R \ln 2 + (C_l - C_S^E) \ln \frac{T_R}{T_E} \qquad (3)$$

where all entropy and temperature values are for fusion, C is the molar heat capacity at constant pressure, and temperature is in Kelvin.[3] Values for entropy in the preceding equation were calculated using

$$\Delta G = \Delta H - T\Delta S \qquad (4)$$

where ΔG equals zero (at equilibrium), and all values are for fusion. The molar free energy of formation for racemic compound from pure crystalline enantiomers was calculated using

$$\Delta G_f^{\phi} = \Delta H_E\left(1 - \frac{T_R}{T_E}\right) - T_R R \ln 2 + (C_l - C_S^E)\left(T_R - T_E - T_R \ln \frac{T_R}{T_E}\right) \qquad (5)$$

where all enthalpy and temperature values are for fusion, C is the molar heat capacity at constant pressure, and temperature is in Kelvin.[3]

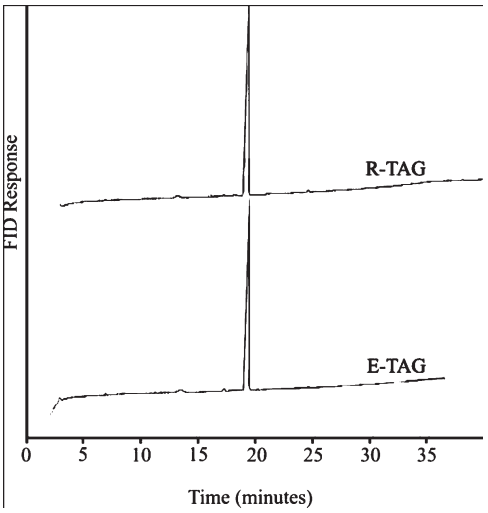

Figure 3. Gas chromatograms for enantiopure 1,2-bisdecanoyl-3-palmitoyl-*sn*-glycerol (E-TAG) and racemic bisdecanoyl-1(3)-palmitoyl-*rac*-glycerol (R-TAG).

RESULTS AND DISCUSSION

For simplicity, enantiopure 1,2-bisdecanoyl-3-palmitoyl-*sn*-glycerol (Figure 2) will occasionally be identified by the letter E or the short form E-TAG, and racemic bisdecanoyl-1(3)-palmitoyl-*rac*-glycerol by the letter R or the short form R-TAG. It is worth noting that the racemic mixture (bisdecanoyl-1(3)-palmitoyl-*rac*-glycerol) is composed of 1,2-bisdecanoyl-3-palmitoyl-*sn*-glycerol and 1-palmitoyl-2,3-bisdecanoyl-*sn*-glycerol (E′ or E′-TAG) in a 1:1 ratio. Consequently, R-TAG could also be identified as 50% E-TAG and 50% E′-TAG in the accompanying figures, tables, and text. For consistency, we will use terminology as defined in Jacques, Collet, and Wilen's book, *Enantiomers, Racemates and Resolutions*.[3]

Chemical and enzymatic methods were compared for the production of monopalmitin; both methods produced pure product at 60.5% yield. Chemical esterification with decanoyl chloride was used to produce both the enantiopure and the racemic TAG from monopalmitin. Subsequent flash chromatography yielded product (E: 74% and R: 49% yield) in very high purity (>99% by GC) (Figure 3). As expected, NMR spectra (^{1}H and ^{13}C) are identical for both enantiopure compound and racemic mixture δ_H = 0.88 (9H, t), 1.26 (48H, m), 1.61 (6H, m), 2.31 (6H, m), 4.21 (4H, m) and 5.27 (1H, m) (Figure 4a). Peaks in the ^{13}C NMR spectrum (Figure 4b) can be assigned as follows: 14.11 (ω-1), 22.69 and 22.72 (ω-2), 24.89 and 24.93 (C3), 29.10 to 29.72 (methylene envelope), 31.89 and 31.95 (ω-3), 34.07 and 34.23 (C2), 62.11 and 68.89 (glycerol), 76.75

dx.doi.org/10.1021/cg101654c |*Cryst. Growth Des.* 2011, 11, 1723–1732

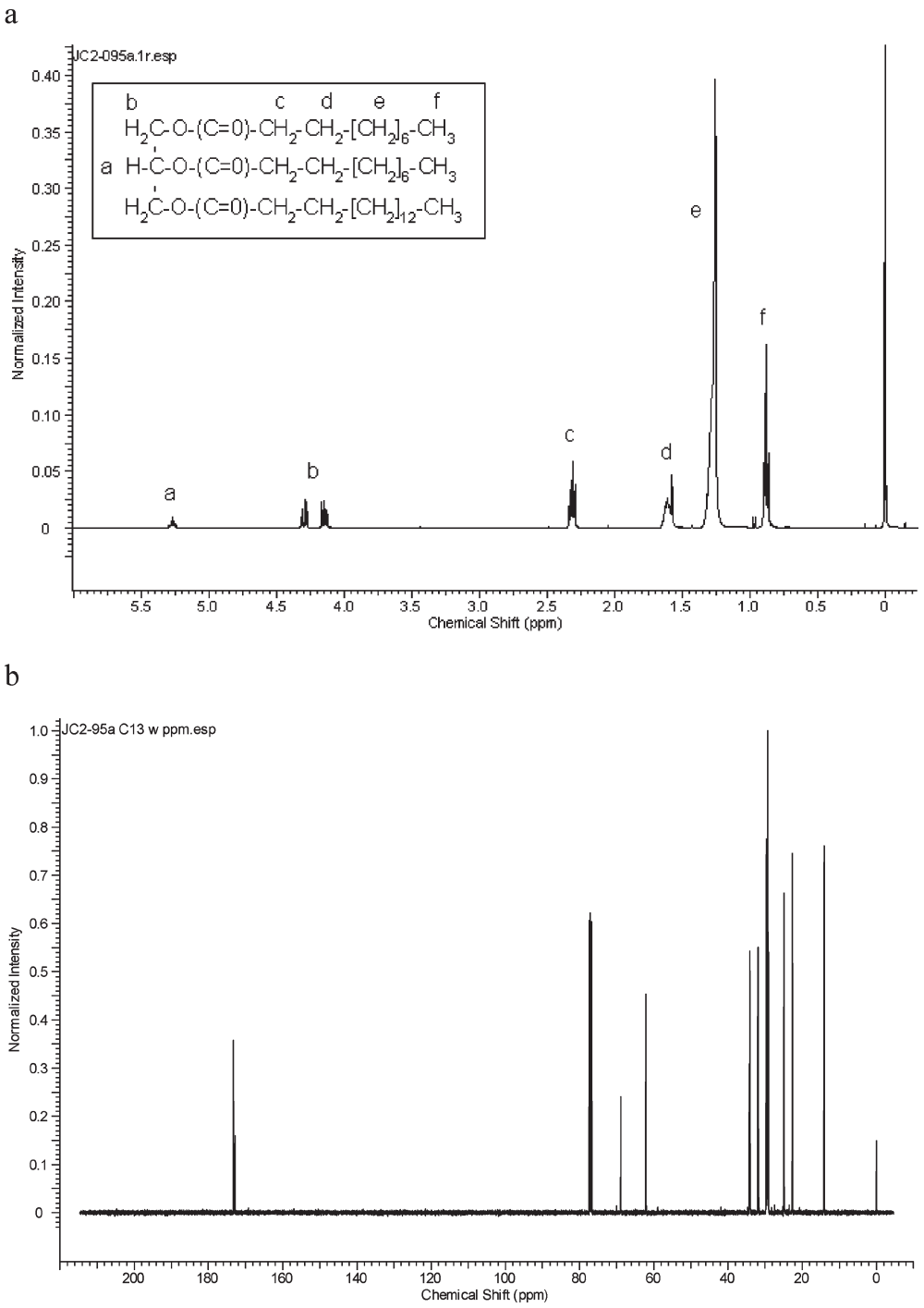

Figure 4. (a) ^{1}H and (b) ^{13}C NMR spectra for enantiopure 1,2-bisdecanoyl-3-palmitoyl-*sn*-glycerol. Peak assignments for ^{1}H are provided in the inset.

to 77.38 (solvent), and finally, 172.87 and 173.28 (carboxyl) according to the scheme laid out by Gunstone.[15]

Infrared spectra for the highest-melting forms of enantiopure compound and racemic mixture were remarkably different (tempering procedure described above). The main differences observed were due to absorbance peaks associated with carboxyl groups and methylene rocking in the acyl chains (Figure 5, Table 1). Carboxyl stretching produces a single absorbance at 1738 cm^{-1} for E-TAG and two separate absorbance peaks at 1730 and 1736 cm^{-1} for R-TAG. While the occurrence of two peaks for β-form R-TAG has not been reported previously, it appears modern FTIR spectrophotometers are capable of resolving the two previously unresolved wavelengths. This was demonstrated by recording an FTIR spectrum for an analytical standard of β-form tripalmitin. Note the two absorbance peaks at 1728 and 1736 cm^{-1} (major and minor, respectively) (Figure 5). R-TAG has a single absorbance (due to methylene rocking) around 720 cm^{-1} indicating methylene groups in adjacent acyl chains are packed in a triclinic parallel arrangement (β polymorph), whereas E-TAG has a smaller peak at 720 cm^{-1} and a plateau from 721 to 727 cm^{-1} indicating orthorhombic perpendicular packing for acyl chains (β' polymorph) (Figure 5).[21]

dx.doi.org/10.1021/cg101654c |*Cryst. Growth Des.* 2011, 11, 1723–1732

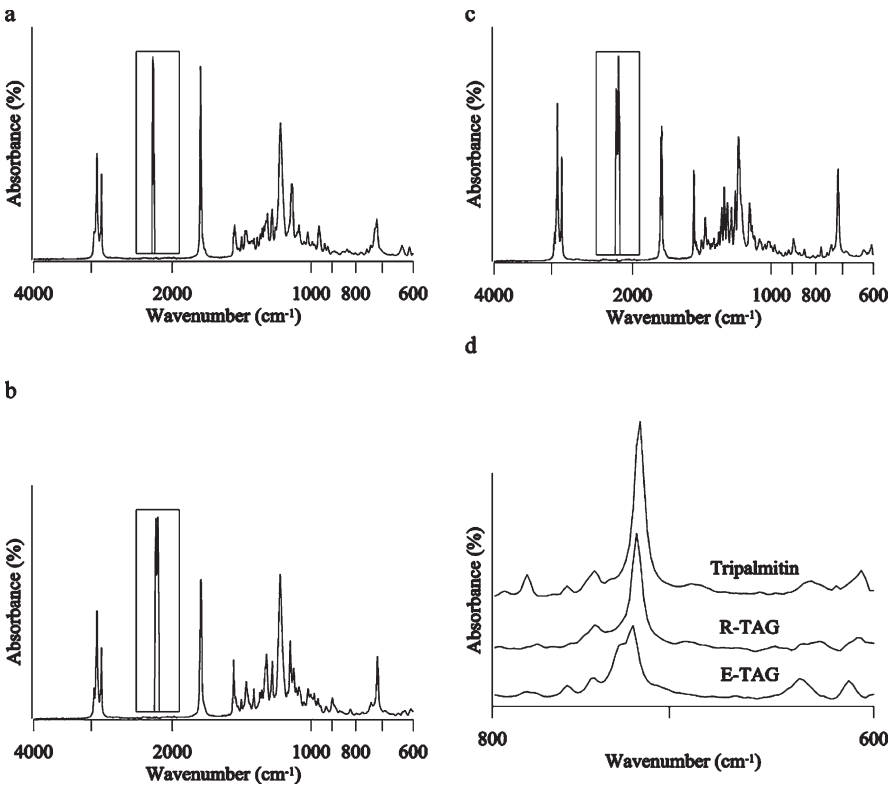

Figure 5. Infrared spectra for (a) enantiopure 1,2-bisdecanoyl-3-palmitoyl-*sn*-glycerol (E-TAG) with inset emphasizing single absorbance band at 1738 cm^{-1}; (b) racemic bisdecanoyl-1(3)-palmitoyl-*rac*-glycerol (R-TAG) with inset emphasizing absorbance bands at 1730 and 1736 cm^{-1}; (c) tripalmitin with inset emphasizing absorbance bands at 1728 and 1736 cm^{-1}; and (d) comparison of region around 720 cm^{-1}.

Table 1. Main Infrared Absorbances for 1,2-Bisdecanoyl-3-palmitoyl-*sn*-glycerol (E) and Bisdecanoyl-1(3)-palmitoyl-*rac*-glycerol (R)[21]

wavenumber (cm^{-1})	description
2849 and 2914	C−H stretch for acyl chain and glycerol backbone
E: 1738	C═O stretch; one peak; (E ≈ R)
R: 1730 and 1736	C═O stretch; two peaks
1471	strongest C−H deformation and wagging band (R > E)
1300−1400	C−H deformation and wagging bands
1167	C−O stretching (E ≈ R)
1142 − 1186	C−O stretching bands
870−1150	C−C stretch and C−H rocking vibrations
720	methylene rocking vibrations E: 720 cm^{-1} and plateau 721 to 727 cm^{-1} (β' polymorph) R: 720 cm^{-1} sharp single peak (β polymorph)

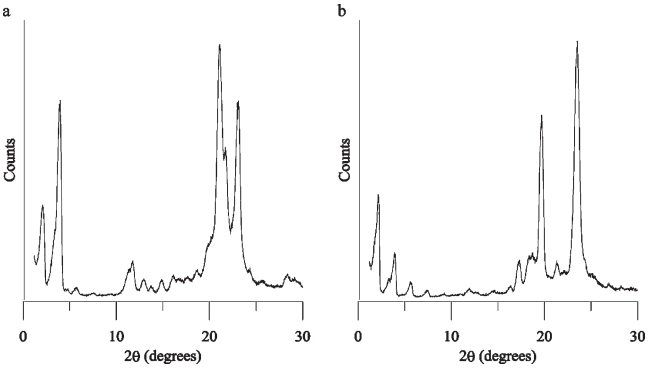

Figure 6. X-ray powder diffraction patterns for (a) enantiopure 1,2-bisdecanoyl-3-palmitoyl-*sn*-glycerol and (b) racemic bisdecanoyl-1(3)-palmitoyl-*rac*-glycerol.

As already mentioned, samples were tempered extensively to ensure the most thermodynamically stable form was obtained. X-ray powder diffraction results for the highest-melting forms of enantiopure and racemic TAG were markedly different (Figure 6, Table 2). In fact, E- and R-TAG have different polymorphic tendencies (β'- and β-tending, respectively). Main peaks in the WAXS region for the enantiopure compound are similar to those generally expected for TAG in the β' polymorph and approximately 0.15 Å lower than previously reported values for β'-form of R-TAG (bisdecanoyl-1(3)-palmitoyl-*rac*-glycerol in Table 2). Discrepancies between experimental and literature values may be due to differences in purity (see discussion of melting points below) or methodology (improved resolution for XRD measurement). Coupled with the FTIR spectra discussed previously, this indicates the highest melting form for E-TAG is β'.

Main peaks in the WAXS region for the racemic mixture are similar to characteristic values and values previously reported for TAG in the β polymorph (Table 2). For instance, values and spectra (cf. Figure 6a in ref 24) from Kodali, Atkinson, and Small for β-form 1,2-dipalmitoyl-3-decanoyl-*sn*-glycerol are a close match to the experimentally determined values and spectrum (Table 2, Figure 6b). Similarly, values reported for β-form bisdecanoyl-1(3)-palmitoyl-*rac*-glycerol by Malkin[10] in 1954 determined from photographic film are all from 0.06 to 0.12 Å

dx.doi.org/10.1021/cg101654c |*Cryst. Growth Des.* 2011, 11, 1723–1732

Table 2. Main X-ray Diffraction Bands for 1,2-Bisdecanoyl-3-palmitoyl-*sn*-glycerol (E) and Bisdecanoyl-1(3)-palmitoyl-*rac*-glycerol (R) with Relevant Data from the Literature

β'-forms	short-spacings (Å)						source
1,2-bisdecanoyl-3-palmitoyl-*sn*-glycerol	3.86 vs		4.09[a]			4.20 vs	experimental
bisdecanoyl-1(3)-palmitoyl-*rac*-glycerol	3.94					4.35	ref 10
dilauroyl-1(3)-stearoyl-*rac*-glycerol	3.94 s			4.17 m		4.30 m	ref 22
dihexanoyl-1(3)-palmitoyl-*rac*-glycerol	3.74 m		4.03s			4.22 s	ref 23
dihexanoyl-1(3)-stearoyl-*rac*-glycerol	3.69 m					4.15 s	ref 23
characteristic β'	3.8					4.2	refs 5, 7, 8
β-forms	short-spacings (Å)						source
bisdecanoyl-1(3)-palmitoyl-*rac*-glycerol	3.78 vs		4.16 vw	4.51 vs	4.7 w		experimental
bisdecanoyl-1(3)-palmitoyl-*rac*-glycerol	3.84 s		4.27 w	4.60 s	4.85 w	5.26 w	ref 10
1,2-dipalmitoyl-3-decanoyl-*sn*-glycerol	3.8 s		4.13 w	4.5 s	4.7 w		ref 24
dilauroyl-1(3)-stearoyl-*rac*-glycerol	3.84 s			4.60 s			ref 22
dihexanoyl-1(3)-stearoyl-*rac*-glycerol	3.93 s	4.11 m	4.38 m	4.54s	4.68 m	5.28 m	ref 23
characteristic β	3.7 s	3.9 s		4.6 s			refs 7, 8
characteristic β	3.8	3.9		4.6			ref 5
characteristic β	3.8			4.6			ref 6

[a] Shoulder.

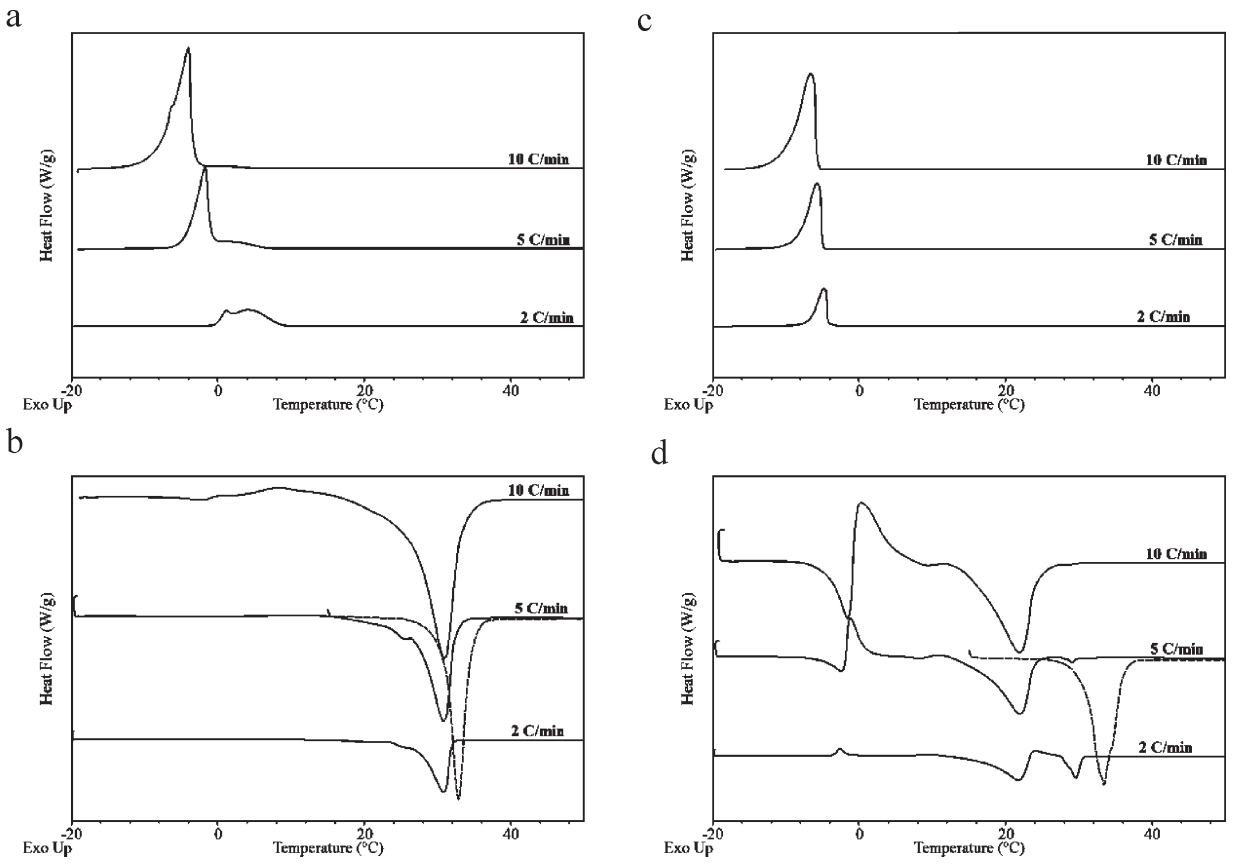

Figure 7. Differential scanning calorimetry curves for the (a) crystallization and (b) melting of enantiopure 1,2-bisdecanoyl-3-palmitoyl-*sn*-glycerol and the (c) crystallization and (d) melting of racemic bisdecanoyl-1(3)-palmitoyl-*rac*-glycerol. Dashed line distinguishes the high-melting form (tempered samples), and solid lines delineate cooling/heating cycles starting with completely melted samples.

more than our values indicating, perhaps, an error in measurement (given the technology at the time; cf. ~0.15 Å difference for β' values discussed above). Likewise, powder diffraction data for R-TAG corresponds with reported short-spacings for dilauroyl-1(3)-stearoyl-*rac*-glycerol and dihexanoyl-1(3)-stearoyl-*rac*-glycerol in the β form.[22,23] Taken with the FTIR data discussed previously, this indicates the highest-melting form for R-TAG is β.

dx.doi.org/10.1021/cg101654c |*Cryst. Growth Des.* 2011, 11, 1723–1732

Table 3. Crystallization and Melting Data[a] for Enantiopure and Racemic Triacylglycerols

	enantiopure 1,2-bisdecanoyl-3-palmitoyl-*sn*-glycerol						
	crystallization 1			crystallization 2			total
	T_e (°C)	T_p (°C)	ΔH_f (kJ/mol)	T_e (°C)	T_p (°C)	ΔH_f (kJ/mol)	ΔH_f (kJ/mol)
2 °C/min		1.18	20.22	8.56	4.01	59.90	80.13
5 °C/min	−0.98	−1.75	63.99	6.84	0.23	10.35	74.39
10 °C/min	−3.49	−4.04	66.54	4.92	−1.9	1.68	68.27
	melting 1			melting 2			total
	T_e (°C)	T_p (°C)	ΔH_f (kJ/mol)	T_e (°C)	T_p (°C)	ΔH_f (kJ/mol)	ΔH_f (kJ/mol)
5 °C/min[b]				30.99	32.90	94.55	94.55
2 °C/min				27.33	30.87	84.09	84.09
5 °C/min	22.03	25.68	14.61	27.07	30.81	67.56	82.17
10 °C/min				26.35	30.95	79.05	79.05
	racemic bisdecanoyl-1(3)-palmitoyl-*rac*-glycerol						
	crystallization						
	T_e (°C)		T_p (°C)			ΔH_f (kJ/mol)	
2 °C/min	−4.31		−4.76			58.89	
5 °C/min	−5.05		−5.75			54.86	
10 °C/min	−5.79		−6.62			54.01	
	melting 1			melting 2			total
	T_e (°C)	T_p (°C)	ΔH_f (kJ/mol)	T_e (°C)	T_p (°C)	ΔH_f (kJ/mol)	ΔH_f (kJ/mol)
5 °C/min[b]				30.97	33.38	104.4	104.4
2 °C/min	16.99	21.82	61.98	28.15	29.6	18.93	80.9
5 °C/min	16.34	21.92	68.27	28.32	29.07	1.22	69.48
10 °C/min	15.54	21.92	58.56				58.56

[a] Extrapolated onset (T_e) and peak maximum (T_p) temperatures. [b] High-melting form.

Experimental long-spacing values for E-TAG (48.22 Å) and R-TAG (49.57 Å) were also different. The value for R-TAG (49.57 Å) matches previously reported literature values for β-form R-TAG of 49.7 Å.[10,22] Long-spacing values confirm a 3L structure for both E- and R-TAG as predicted based on the difference in acyl chain length (>4 carbons).[9] The experimental value for β-form R-TAG (49.57 Å) corresponds with the value calculated using the equation $L = (n + 6.71)0.116$ nm ($n = 36$; L = 49.54 Å) derived for saturated TAG in a 3L β-form conformation.[6] Consequently, the acyl chain to chain-end plane angle (τ) for the high-melting form (β) of R-TAG is close to 66.4°.

Solid samples in the highest-melting form (see above) were transferred to DSC pans, and an initial melt at 5 °C/min was measured (Table 3; Figure 7). Melting data for both the enantiopure compound and racemic mixture display minor differences (E: T_e = 30.99 °C, T_p = 32.9 °C, ΔH_f = 94.55 kJ/mol; R: T_e = 30.97 °C, T_p = 33.38 °C, ΔH_f = 104.4 kJ/mol). For comparison, melting data for R-TAG in β' and β form (32 and 35 °C, respectively)[10] have been reported previously. However, this data predates the first commercial DSC (1964), and methodologies for determining purity of starting materials and final products were not fully developed at that time.[25] By the same token, Ravich and Tsurinov's (1946) determination of ΔH_f for R-TAG (123.1 kJ/mol) should, no doubt, be viewed with similar caution.[7,26]

While there is little difference in melting temperature and ΔH_f for high-melting forms of E- and R-TAG, differences in polymorphic behavior are evident from a comparison of crystallization and melting curves collected at 2, 5, and 10 °C/min (Figure 7). At least one additional polymorph is evident in the crystallization curves for E-TAG, whereas melting curves display minimal polymorphism (some minor peaks). In contrast, R-TAG crystallization curves are free of polymorphic occurrences, while the corresponding melting curves display intense polymorphism. These differences are also evident in the compiled crystallization and melting data derived from these curves (Table 3). Data in the table for R-TAG melting includes only the two highest-melting forms (β' and β), although a further low-melting form (α) is visible in melting curves (Figure 7).

The DSC melting curves for binary mixtures of 1,2-bisdecanoyl-3-palmitoyl-*sn*-glycerol and bisdecanoyl-1(3)-palmitoyl-*rac*-glycerol in the highest-melting form have been plotted together to facilitate comparison (Figure 8). These DSC melting curves are used to identify the most thermodynamically stable polymorphs for the phase diagram.

In addition to those for the high-melting form (Figure 8), DSC melting curves for binary mixtures of 1,2-bisdecanoyl-3-palmitoyl-*sn*-glycerol and bisdecanoyl-1(3)-palmitoyl-*rac*-glycerol crystallized and melted at 2, 5, and 10 °C are presented in Figures 9, 10 and 11, respectively. These DSC cooling/heating cycles were used to

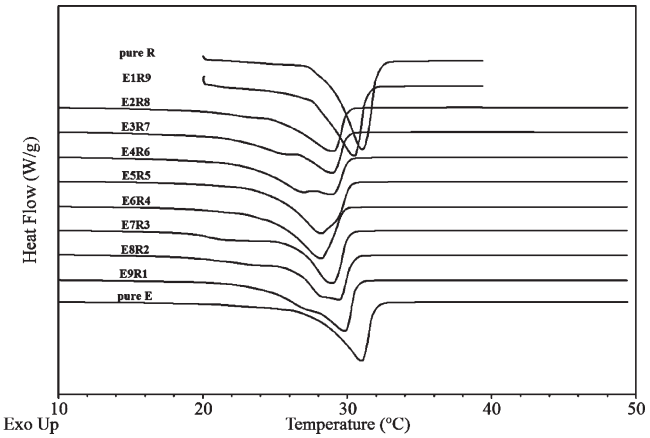

Figure 8. DSC curves for the high-melting form of binary blends of enantiopure 1,2-bisdecanoyl-3-palmitoyl-*sn*-glycerol and racemic bisdecanoyl-1(3)-palmitoyl-*rac*-glycerol. Samples were stored at 22 °C for 3 days prior to analysis and then melted at 2 °C/min. E and R in curve labels refer to the relative proportions of the enantiopure compound and the racemic mixture.

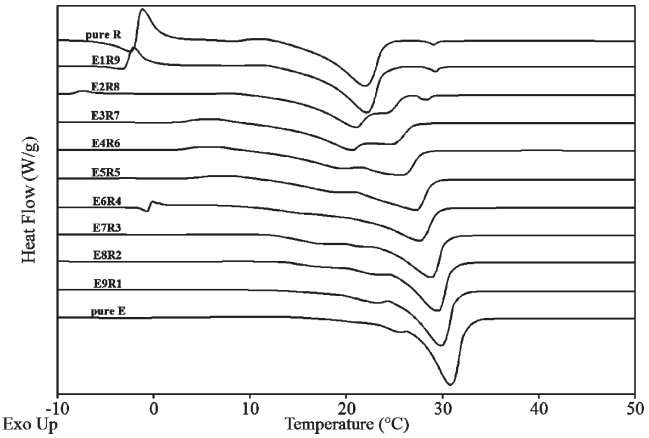

Figure 10. DSC melting curves for binary blends of enantiopure 1,2-bisdecanoyl-3-palmitoyl-*sn*-glycerol and racemic bisdecanoyl-1(3)-palmitoyl-*rac*-glycerol. Samples were melted and held at 80 °C for 5 min prior to analysis. Samples were cooled from 80 °C to −20 at 5 °C/min and then melted at 5 °C/min. E and R in curve labels refer to the relative proportions of the enantiopure compound and the racemic mixture.

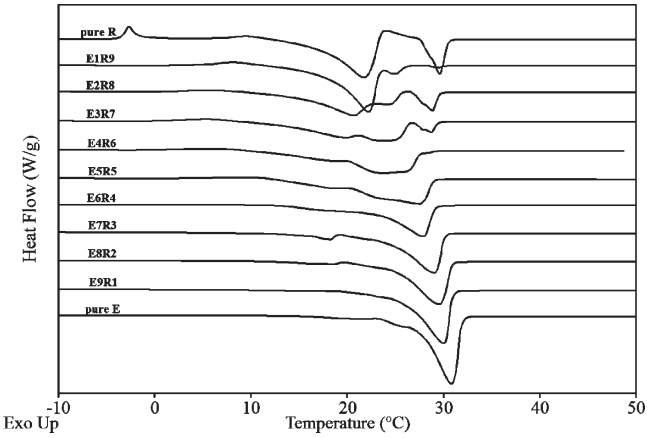

Figure 9. DSC melting curves for binary blends of enantiopure 1,2-bisdecanoyl-3-palmitoyl-*sn*-glycerol and racemic bisdecanoyl-1(3)-palmitoyl-*rac*-glycerol. Samples were melted and held at 80 °C for 5 min prior to analysis. Samples were cooled from 80 °C to −20 at 2 °C/min and then melted at 2 °C/min. E and R in curve labels refer to the relative proportions of the enantiopure compound and the racemic mixture.

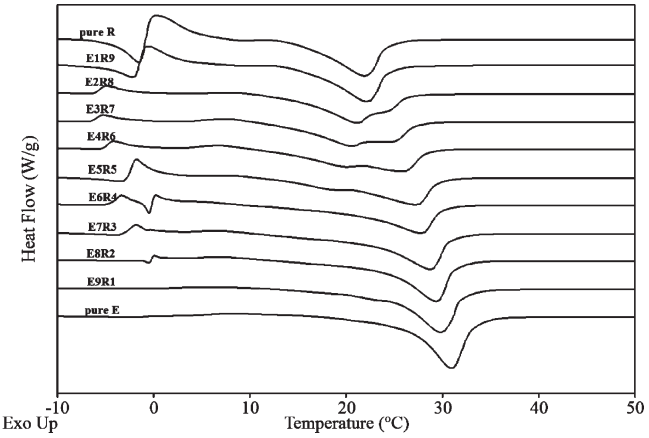

Figure 11. DSC melting curves for binary blends of enantiopure 1,2-bisdecanoyl-3-palmitoyl-*sn*-glycerol and racemic bisdecanoyl-1(3)-palmitoyl-*rac*-glycerol. Samples were melted and held at 80 °C for 5 min prior to analysis. Samples were cooled from 80 °C to −20 at 10 °C/min and then melted at 10 °C/min. E and R in curve labels refer to the relative proportions of the enantiopure compound and the racemic mixture.

identify the major metastable and stable polymorph. It is interesting to note that for samples rich in the enantiopure compound (E7R3 to pure E), one main peak with few minor peaks (due to metastable forms) are observed. In contrast, samples rich in racemic mixture (pure R to E6R4) display numerous endothermic and exothermic peaks due to the occurrence of metastable forms. Perhaps most notable among these are the peaks around −3 °C caused by the melting of α-form solids and the subsequent crystallization of solids in the β'-form. Also worth noting is the absence (and near absence) of the high-melting form in racemic and near racemic mixtures heated at 5 and 10 °C/min (Figures 10 and 11).

Melting data derived from the DSC melting curves for binary mixtures crystallized and melted at 2, 5, and 10 °C/min are presented in Table 4. Despite the difference in cooling/heating rate, linear regression for the mean values yields an equation to describe the line (T_p(°C) = −9.2203x + 30.88) with R^2 = 0.9719. On the phase diagram, this line indicates eutectic phase behavior and consequently conglomerate formation for binary mixtures of E- and E′-TAG (both of which are β'-stable) (solid line in Figure 12). Melting data for high-melting forms (solid triangles in Figure 12) departs from the aforementioned trend. For this data the phase diagram shows eutectic behavior between the enantiopure compound and the racemic mixture indicating a racemic compound is formed by E- and E′-TAG. Thus, the unit cell for the solid racemic mixture contains an equal number of E- and E′-TAG molecules in the highest-melting form (β). Despite the relative scarcity of conglomerate systems, similar behavior (monotropy with a metastable conglomerate) has been reported for 2,2′-diamino-1,1′-binaphthyl and α-bromocamphor.[3]

The location of the high-melting β-form liquidus is suggested in Figure 12 by a dashed line. Peaks due to the melting of high-melting form are smaller in cooling/heating cycles (minor peaks in Figures 9 and 10; open triangles, and diamonds in Figure 12) than the corresponding peaks for tempered samples (major

Table 4. Melting Data (T_p) for Binary Mixtures of 1,2-Bisdecanoyl-3-palmitoyl-*sn*-glycerol (E) and Bisdecanoyl-1(3)-palmitoyl-*rac*-glycerol (R) at Three Different Cooling/Heating Rates

	T_p (°C)				
sample	2 °C/min	5 °C/min	10 °C/min	mean	SD
pure E	30.87	30.81	30.95	30.88	0.07
E9R1	30.04	29.80	29.79	29.88	0.14
E8R2	29.60	28.47	29.35	29.47	0.13
E7R3	29.06	28.74	28.72	28.84	0.19
E6R4	28.01	27.53	27.76	27.77	0.24
E5R5	27.55	27.24	27.17	27.32	0.20
E4R6	23.77	25.75	25.75	25.09	1.14
E3R7	23.76	24.67	24.20	24.21	0.46
E2R8	24.19	23.02	21.11	22.77	1.55
E1R9	22.26	22.09	22.09	22.15	0.10
pure R	21.82	21.93	21.92	21.89	0.06

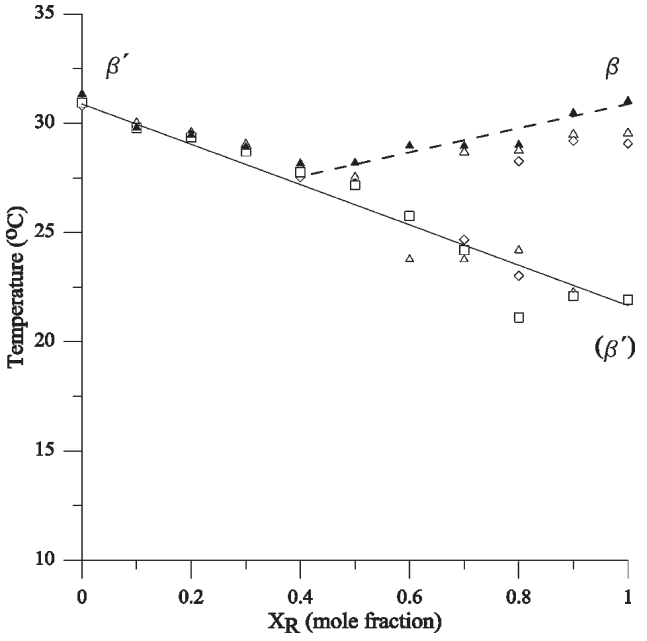

Figure 12. Liquidus data (T_p) for stable and metastable polymorphs of binary mixtures of 1,2-bisdecanoyl-3-palmitoyl-*sn*-glycerol (E-TAG) and bisdecanoyl-1(3)-palmitoyl-*rac*-glycerol (R-TAG). Triangles are for data collected at 2 °C/min, diamonds for 5 °C/min, and squares for 10 °C/min. Solid symbols represent melting data for tempered samples, and open symbols represent data obtained from cooling/heating cycles on melted samples. Solid line was derived by linear regression on mean data, and the dashed line is the suggested high-melting liquidus.

peaks in Figure 8; solid triangles in Figure 12). As a result, T_p for these peaks appears below the dashed line and below T_p for tempered samples in Figure 12. Only peaks associated with the melting of the main stable and metastable form were plotted on this occasion. While this provides sufficient information for an initial characterization; complete characterization of this and similar systems will take considerable time and effort.

For the metastable conglomerate the experimentally determined melting point depression (mean value of 8.99 °C based on data in Table 4) is far more than the theoretical value calculated (5.64 °C) using the Hildebrand equation (eq 1). The difference between calculated and experimental values may be due to the presence of solids with different polytypism in R-TAG (i.e., 2L, 3L, or both). Whereas pure β'-form E-TAG is in a 3L configuration (determined by SAXS above), R-TAG probably crystallizes in a metastable 2L form first and then undergoes a transition to the 3L structure (similar to dilauroyl-1(3)-stearoyl-*rac*-glycerol). As already mentioned, dilauroyl-1(3)-stearoyl-*rac*-glycerol crystallizes in metastable β'_2 and β'_3 forms (T_m = 31 and 38 °C respectively). Lutton reports that the β'_2 form was obtained first, in accordance with Ostwald's rule, and after approximately 10 min at 32 °C the β'_3 form was obtained.[22]

The stability of the racemic compound versus the conglomerate can be calculated using eqs 2−5. For the following calculations, the third or fourth term (in eqs 2, 3, and 5) was regarded as negligible and ignored since differences in temperature and heat capacity are small.[3] The molar enthalpy of formation for the racemic compound from pure crystalline enantiomers (−9.85 kJ/mol by eq 2) indicates formation of the racemic compound is exothermic.[3] The molar entropy of formation for the racemic compound from pure crystalline enantiomers, calculated using eqs 3 and 4, is −26.6 J/(mol K). The molar free energy of formation for the racemic compound from pure crystalline enantiomers, calculated using eq 5 is −1.75 kJ/mol. Thus, formation of the racemic compound is favored slightly over formation of the conglomerate for racemic mixtures.

In conclusion, investigation of phase behavior indicates blends of 1,2-bisdecanoyl-3-palmitoyl-*sn*-glycerol and 1-palmitoyl-2,3-bisdecanoyl-*sn*-glycerol form a metastable conglomerate (in the β' polymorph) and a stable racemic compound (in the β polymorph). In addition, the most thermodynamically stable polymorph for enantiopure 1,2-bisdecanoyl-3-palmitoyl-*sn*-glycerol and by analogy 1-palmitoyl-2,3-bisdecanoyl-*sn*-glycerol was β'. Thus, for the subject compounds, molecules of opposite enantiomers are mutually immiscible in the β'-form and matched (by necessity) in the unit cell of the β-form. This demonstrates the importance of stereochemistry in understanding the polymorphism and crystallization behavior of TAG.

AUTHOR INFORMATION

Corresponding Author

*Tel: 519-824-4120 x54327. E-mail: rlencki@uoguelph.ca.

ACKNOWLEDGMENT

Financial support for this project was provided by National Sciences and Engineering Research Council of Canada; we are grateful for their generosity. Thanks to ACD (Toronto) for their free chemical structure drawing and NMR analysis software (Chemsketch, 3D Viewer and 1D NMR Processor). Thanks also to Japan VAM & POVAL Co., Ltd. for their donation of vinyl esters of fatty acids.

REFERENCES

(1) Gresti, J.; Bugaut, C.; Maniongui, C.; Bezard, J. *J. Dairy Sci.* **1993**, *76*, 1850–1869.

(2) Loh, S. K.; Choo, Y.-M. *J. Oil Palm Res.* **2003**, *15* (1), 6–11.

(3) Jacques, J.; Collet, A.; Wilen, S. H. *Enantiomers, Racemates and Resolutions*; John Wiley and Sons: New York, 1981.

(4) Sato, K.; Ueno, S. Molecular Interactions and Phase Behavior of Polymorphic Fats. In *Crystallization Processes in Fats and Lipid Systems*; Garti, N., Sato, K., Eds.; Marcel Dekker, Inc.: New York, 2001; pp 177−288.
(5) Sato, K.; Ueno, S. Polymorphism in Fats and Oils. In *Bailey's Industrial Oil and Fat Products*, 6th ed.; Shahadi, F., Ed.; John Wiley & Sons, Inc.: Hoboken, NJ, 2005; Vol. 1, pp 77−120.
(6) van Soest, T. C.; de Jong, S.; Roijers, E. C. *J. Am. Oil Chem. Soc.* **1991**, *67* (7), 415–423.
(7) Hagemann, J. W. Thermal Behavior and Polymorphism of Acylglycerides. In *Crystallization and Polymorphism of Fats and Fatty Acids*; Garti, N., Sato, K., Eds.; Marcel Dekker, Inc.: New York, 1988; pp 9−95.
(8) Kodali, D. R.; Atkinson, D.; Redgrave, T. G.; Small, D. M. *J. Am. Oil Chem. Soc.* **1984**, *61* (6), 1078–1084.
(9) Lutton, E. S. *J. Am. Oil Chem. Soc.* **1950**, *July*, 276–281.
(10) Malkin, T. *Prog. Chem. Fats Lipids* **1954**, *2*, 1–50.
(11) Gaffney, P. R. J.; Reese, C. B. *J. Chem. Soc., Perkin Trans.* **2001**, *1*, 192–205.
(12) Craven, R. J.; Lencki, R. W. *J. Am. Oil Chem. Soc.* **2010**, *87* (11), 1281–1291.
(13) Yu, C. C.; Lee, Y.-S.; Cheon, B. S.; Lee, S. H. *Bull. Korean Chem. Soc.* **2003**, *24* (8), 1229–1231.
(14) Halldorsson, A.; Magnusson, C. D.; Haraldsson, G. G. *Tetrahedron* **2003**, *59*, 9101–9109.
(15) Gunstone, F. D. *Chem. Phys. Lipids* **1990**, *56*, 195–199.
(16) Cullity, B. D. *Elements of X-Ray Diffraction*, 2nd; Addison-Wesley Publishing Company, Inc.: Reading, MA, 1978.
(17) Bernstein, J. *Polymorphism in Molecular Crystals*; Oxford University Press: Oxford, 2002.
(18) Hohne, G. W. H.; Hemminger, W. F.; Flammersheim, H. J., *Differential Scanning Calorimetry*, 2nd ed.; Springer-Verlag: New York, 2003.
(19) Laye, P. G. Differential Thermal Analysis and Differential Scanning Calorimetry. In *Principles of Thermal Analysis and Calorimetry*; Haines, P. J., Ed.; Royal Society of Chemistry: Cambridge, U.K., 2002; pp 55−93.
(20) Atkins, P. W. *Physical Chemistry*, 2nd ed.; Oxford University Press: Oxford, 1982.
(21) Chapman, D. *The Structure of Lipids by Spectroscopic and X-ray Techniques: With a Chapter on Separation Techniques Including Thin Layer and Gas Liquid Chromatography*; Methuen and Co Ltd: London, 1965.
(22) Lutton, E. S. *J. Am. Chem. Soc.* **1948**, *70* (1), 248–254.
(23) Jackson, F. L.; Lutton, E. S. *J. Am. Chem. Soc.* **1952**, *74* (19), 4827–4829.
(24) Kodali, D. R.; Atkinson, D.; Small, D. M. *J. Phys. Chem.* **1989**, *93* (11), 4683–4691.
(25) Nutter, B. *Catalog 2009/2010*; Nu-Chek Prep, Inc.: Elysian, MN, 2009.
(26) Ravich, G.; Tsurinov, C. *Acta Physicochim. URSS* **1946**, *21*, 321, as cited in ref 7.